Probe Report: Formylpeptide Receptor-Like-1 Antagonist

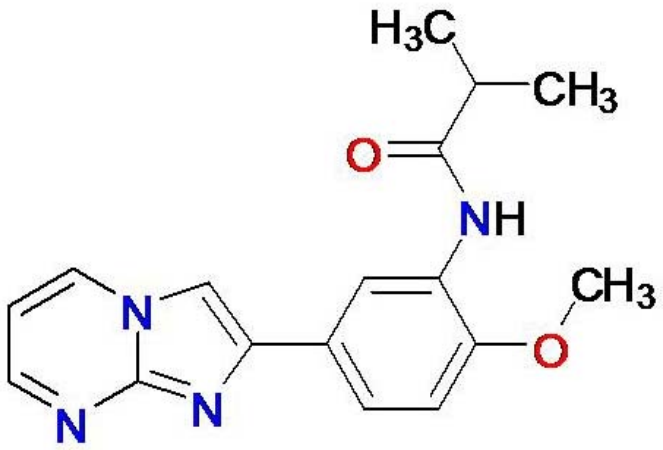

FPR Antagonist Probe **BB-V-115 (**PubChem CID **6622773)**

Project Title: Assay for Formylpeptide Receptor Family Ligands
Grant Number: NIH 1R03MH076381-01

Screening Center Name: New Mexico Molecular Libraries Screening Center
Principal Investigator of Screening Center: Larry A. Sklar, Ph.D.

Assay Submitter and Institution: Bruce S. Edwards, Ph.D, University of New Mexico

PubChem Assay Identifiers (AIDs): 440, 441, 519, 520, 698, 762, 763, 765, 766, 1061, 1202 (Summary)

Assay Target: Human Formylpeptide Receptor-Like-1 (FPRL1)

Probe PubChem Compound Identifier: 6622773

Mode of Action: FPRL1 Ligand and Antagonist

Summary

This report describes a novel small molecule probe (**BB-V-115,** PubChem CID **6622773)** directed against the human formylpeptide receptor-like-1 (FPRL1), a G-protein coupled receptor implicated in anti-bacterial inflammatory responses and malignant glioma metastasis. The molecule displaced a high-affinity, fluorescent ligand from FPRL1 with an inhibition constant (K_i) of 269 ± 51 nM (mean ± SEM). **BB-V-115** exhibited ~13-fold greater potency in ligand displacement experiments in a head-to-head comparison with C7, the recently reported small molecule FPRL1 antagonist. It also exhibited a 20-fold difference in K_i for FPRL1 *vs* FPR while C7 exhibited only a 1.4-fold difference. **BB-V-115** was determined to be a selective antagonist for FPRL1 *vs* FPR by virtue of its ability

to inhibit intracellular calcium responses elicited by high affinity FPRL1 but not FPR ligands. Thus, BB-V-115 is the most potent and selective small molecule FPRL1 antagonist reported to date.

Background/Significance

Formyl peptide receptors. The G-protein coupled formylpeptide receptor (FPR) was one of the originating members of the chemoattractant receptor superfamily (1, 2). N-formylated peptides such as fMLF are high affinity FPR ligands that trigger a variety of biologic activities in myeloid cells, including chemokinesis, chemotaxis, cytokine production and superoxide generation (3-7). Since such peptides are derived from bacterial or mitochondrial proteins (8-11), it has been proposed that a primary FPR function is to promote trafficking of phagocytic myeloid cells to sites of infection and tissue damage where they exert anti-bacterial effector functions and clear cell debris. In support of this hypothesis, mice lacking a known murine FPR variant were more susceptible to bacterial infections (12). The glucocorticoid-regulated protein, annexin I (lipocortin I), was recently identified as another protein of host origin that is a specific agonist for human FPR (13). FPR have also been proposed as prospective targets for therapeutic intervention against malignant gliomas (14).

Two additional human genes have been reported to encode FPR variants, FPRL1 and FPRL2 (FPR-like 2)(15-18). FPRL1 shares 69% identity at the amino acid level with FPR and is, like FPR, a seven-transmembrane, G-protein-coupled receptor (GPCR) (3, 19). FPRL2 encodes a receptor that has 56% and 83% amino acid sequence identity to FPR and FPRL1, respectively. Although even micromolar levels of N-formyl peptides such as fMLF only weakly activate FPRL1 (17), a number of host-derived FPRL1 agonists have been identified that are associated with pathophysiological settings. These include amyloidogenic proteins, serum amyloid A (6, 20) and A β_{42} (21), and a prion protein fragment, PrP1206-26 (22), which are involved in chronic inflammation-associated systemic amyloidosis (23), Alzheimer's disease (24, 25), and prion diseases (22, 26), respectively. Since infiltration of activated mononuclear phagocytes is a common feature, cells responding to FPRL1 ligands may contribute to the inflammatory pathology observed in the diseased tissues (7, 27, 28). Other FPRL1 agonists include an enzymatic cleavage fragment of the neutrophil granule derived cathelicidin (29), and a NADH dehydrogenase subunit peptide fragment (30). Moreover, HIV-1 envelope proteins contain domains capable of interacting with either or both FPR and FPRL1 (31-33).

Of the three FPR family members, only FPRL2 has a highly restricted profile, expressed only in monocytes (34). More broadly distributed, FPR is expressed in neutrophils, monocytes, hepatocytes, immature dendritic cells. astrocytes, microglial cells, and the tunica media of coronary arteries (35-38). FPRL1 is expressed in an even greater variety of cell types including phagocytic leukocytes, hepatocytes, epithelial cells, T lymphocytes, neuroblastoma cells, astrocytoma cells, and microvascular endothelial cells (17, 19, 27, 39, 40). In addition, a recent study has documented expression of both FPR and FPRL1 on normal human lung and skin fibroblasts (33). The diverse tissue expression of these receptors suggests the possibility of as yet unappreciated complexity

in the innate immune response and perhaps other unidentified functions for the receptor family.

Known Non-Peptide FPRL1 Antagonist Ligands

To date, whereas a number of small molecule agonists for FPRL1 have been identified (41,42), there has only been one recent report of an antagonist, designated **C7**, that exhibited an IC_{50} of 6.7 μM (47). Our screening center synthesized C7 and determined it to have an IC_{50} of 8.4 μM and corresponding K_i of 2.2 μM in our ligand displacement assay.

Assay Descriptions

Single point HTS assays. The single point HTS assay used flow cytometry to measure test compound competition with a high-affinity fluorescent ligand for binding to human FPR. The assay was performed in a "duplex" format in which U937 cells expressing FPR were tested together with a Rat Basophilic Leukemia (RBL) cell line that expressed the related receptor, FPRL1. The FPR-expressing cells were stained with a red-fluorescent dye, FURA-red, to allow them to be distinguished from the FPRL1-expressing cells during flow cytometric analysis.

A fluorescein label was conjugated to the lysine residue of the peptide, WKYMVm (WPep), to produce a fluorescent ligand (WPep-FITC) that bound FPR and FPRL-1 with high affinity. Dissociation constants (K_d) for binding of WPep-FITC to FPR and FPRL1 were determined to be 1.2 nM and 1.8 nM, respectively. WPep-FITC was used as the fluorescent ligand in the duplex FPR-FPRL1 assay to determine compound activity for both receptors. **A separate probe report has been filed that documents the detailed quantitative characterization of WPep-FITC binding to FPR and FPRL1. The report is entitled "Fluorescent Cross-Reactive FPR/FPRL1 Hexapeptide Ligand".**

For assay performance, additions to wells were in sequence as follows: 1) test compounds and control reagents (5 μL/well); 2) a combination of FPR- and FPRL1-expressing cell lines (10^7/mL each, 5 μL/well); 3) (after 30 min, 4º C incubation) fluorescent peptide (5 μL/well). After an additional 45 min, 4º C incubation, plates were immediately analyzed by flow cytometry. The assay response range was defined by replicate control wells containing unlabeled receptor-blocking peptide (positive control) or buffer (negative control). fMLFF (4Pep) was used as the FPR-blocking peptide, unlabeled WPep as the FPRL1-blocking peptide.

The assay was homogeneous in that cells, compounds and fluorescent peptide were added in sequence and the wells subsequently analyzed without intervening wash steps. The HyperCyt high throughput flow cytometry platform (43, 44) was used to sequentially sample cells from wells of 384-well microplates (2 μL/sample) for flow cytometer presentation at a rate of 40 samples/min. The resulting time-resolved data files were analyzed with IDLeQuery software to determine compound activity in each well.

Test compound inhibition of fluorescent peptide binding was calculated as

%Inhibition = 100 x [1 - (MFI_test - MFI_PC)/(MFI_NC - MFI_PC)]

in which MFI_Test, MFI_PC and MFI_NC represent the median fluorescence intensity of cells in wells containing test compound, the average MFI of cells in positive control wells and the average MFI of cells in negative control wells, respectively.

Dose response assays. Dose response assays were performed essentially as described for single point assays except that test compounds were hit-picked at a 10 mM concentration (unless otherwise indicated) in DMSO and serially diluted 1:3 eight times for a total of nine different test compound concentrations. Final compound dilution factors in the assay ranged from 1:984,150 to 1:150. For a starting concentration of 10 mM this corresponded to a concentration range of 10.2 nM to 66.7 µM.

In an individual dose response experiment, each compound was tested in duplicate to result in 18 data points. Some compounds were tested in more than one dose-response experiment. The number of data points for dose response curves ranged from 18 (a single experiment) to 90 (5 experiments). In some cases individual data points were determined to be statistical outliers and were eliminated from the analysis.

Ligand competition curves were fitted by Prism® software (GraphPad Software, Inc., San Diego, CA) using nonlinear least-squares regression in a sigmoidal dose response model with variable slope, also known as the four parameter logistic equation. Two parameters, the top and bottom of the fitted curves, were fixed at 100 and 0, the expected upper and lower boundaries of normalized data. Curve fit statistics were used to determine the concentration of added test compound competitor that inhibited fluorescent ligand binding by 50 percent (IC_{50}, µM), the low and high boundaries of the 95% confidence interval of the IC_{50} estimate, the Hill Slope, and the correlation coefficient (r^2) indicative of goodness-of-fit.

FPRL1 expression ranged from 100,000 to 200,000 receptors per cell in different assays as determined by comparison to standard curves generated with Fluorescein Reference Standard Microbeads (Bangs Laboratories, Fishers, IN). This corresponded to total FPR concentrations of 0.6 to 1.2 nM. To account for effects of possible ligand depletion at the higher receptor concentrations, K_i were calculated from IC_{50} estimates by the method of Munson and Rodbard (45):

$$K_i = K_d \times [y0/(y0+2)] + IC_{50}/\{1 + [p^* \times (y0+2)]/[2 \times K_d \times (y0+1)] + y0\}$$

in which y0 is the initial bound-to-free concentration ratio for the fluorescent ligand, p* is the added concentration of fluorescent ligand and K_d is the dissociation constant of the fluorescent ligand.

The fluorescent Wpep ligand had a K_d of 1.8 nM for FPRL1 and was used at a final concentration of 5 nM.

Intracellular calcium response antagonist assay. Calcium response experiments were done as previously described (41, 46) with minor modifications. U937 cells expressing FPR were resuspended in warm tissue culture medium (10^7 cells in 10 mL) containing 200 nM Fluo4 acetoxymethyl ester (Molecular Probes, Eugene, OR) and incubated at 37º C for 30 minutes, with mixing every 10 minutes. After incubation, Fluo4-loaded cells were washed twice by centrifugation, resuspended in complete HHB medium (110 mM NaCl, 30 mM HEPES, 10 mM KCL, 1mM MgCl2, 10 mM glucose, and 0.1% (v/v) human serum albumin, and 1.5 mM CaCl2), allowed to equilibrate at 37º C for 10 minutes, and stored on ice.

To assess the ability of test compounds to block FPR-induced intracellular calcium responses, Fluo4-loaded cells (1 x 10^6/mL in 100 µL) were first incubated with or without the compound for 8 minutes at 37º C (final concentrations of 0 to 100 µM test compound, 1% v/v DMSO). Cells were next analyzed for 20 seconds in a FACScan™ flow cytometer (BD Biosciences) to establish a baseline for Fluo-4 fluorescence intensity. Finally, a 100 µL volume of HHB containing 0 or 1 nM of fMLFF peptide was manually added and the analysis was reinitiated for an additional 30 seconds. For the duration of data collection the cell suspension was maintained at 37º C and continuously stirred with a magnetic stirbar. Fluo4 fluorescence was excited at 488 nM and its emission intensity analyzed at 530 nm. The median Fluo4 fluorescence intensity (MFI) was determined at 0.6 second intervals, ~500 cells in each interval, throughout the analysis.

The MFI values were summed and averaged for the 20 seconds prior to stimulus addition (Avg_MFI_Base). The MFI values were summed over 50 measurements made during the 30 seconds immediately post-addition to determine the area under the response curve post-addition (AUC_Post). Avg_MFI_Base was multiplied by 50 to obtain a baseline area under the curve estimate (AUC_Base). The response to stimulus was calculated as the difference:

$$\text{AUC_Response} = \text{AUC_Post} - \text{AUC_Base}$$

AUC_Response was calculated for 3 conditions: 1) no test compound present and fMLFF added as stimulus (Rmax), 2) test compound present and fMLFF added as stimulus (Rtest), and 3) test compound present and HHB medium alone added as stimulus (Rmin).

Test compound inhibition of the calcium response was calculated as:

$$\%\ \text{Inhibition} = 100 \times \{1 - [\ (\text{Rtest} - \text{Rmin})\ /\ (\text{Rmax} - \text{Rmin})\ ]\ \}$$

Results of HTS and Secondary Assays

Initially, 24,304 compounds from the NIH Molecular Libraries Small Molecule Repository (MLSMR) were screened to identify 72 FPRL1 ligands that satisfied hit selection criteria (> 30% inhibition of fluorescent ligand binding active compounds (AID 441). Of these, 6 were determined to have probe-like activity (K_i < 10 µM) in follow up dose response assays (AID 520). In parallel FPR single-point and dose response counter screen assays (AIDs 440 and 519, respectively), none of the probe-like test compounds in

FPRL1 assays exhibited measurable levels of FPR ligand binding potency. The compounds with probe-like activity were tested in secondary intracellular calcium response antagonist assays (AID 698) to identify 3 novel and selective small molecule FPRL1 antagonists. For follow up structure activity relationship (SAR) analysis, 2 major chemotype families (families 3 and 4) representing the probe-like FPRL1 ligands were identified. A set of 170 compounds was selected by application of computational screening techniques (2D substructure search) to a 700k subset of the ChemDiv collection of more than 1 million compounds. The compounds were purchased and screened in a primary HTS FPRL-FPRL1 duplex assay to identify 13 active compounds (AID 765), of which 5 had probe-like potency in follow up dose response assays (AID 766). In parallel FPR single-point and dose response counter screen assays (AIDs 763 and 762, respectively), none of the probe-like test compounds in FPRL1 assays exhibited measurable levels of FPR ligand binding potency. All of the 5 probe-like FPRL1 ligands were in family 3, the most potent of which had a Ki of 269 nM (ChemDiv ID, **G856-0334;** PubChem CID **6622773**). The compound was determined to be an antagonist in an intracellular calcium response antagonist assay. This compound was selected for resynthesis and characterization as a novel non-peptide, small molecule FPRL1 antagonist.

Synthesis and Physical Characterization of Probe BB-V-115

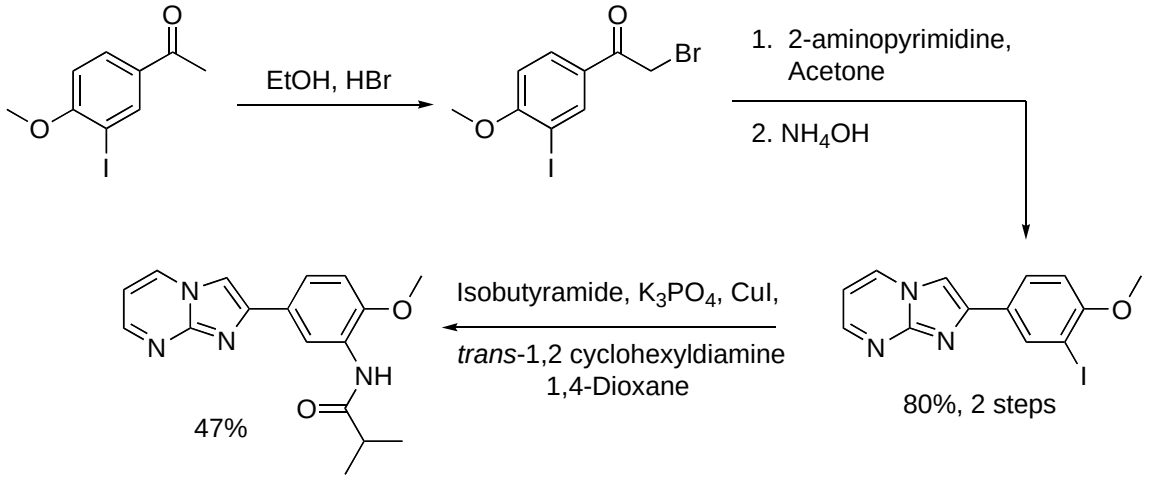

3'-Iodo-4'methoxyacetophenone (276 mg, 1 mmol) was suspended in ethanol (4 mL). Bromine (102 microL, 2 mmols) was added dropwise and stirred at 60°C for 30min. The product was precipitated by the addition of water (20 mL), filtered and dried *in vaccuo*. The product was dissolved in acetone (2 mL), 2-aminopyrimidine was added and stirred at reflux 3h. The reaction was cooled to room temperature, filtered, and the precipitate washed with NH_4OH to give 2-(2'-Iodo-4'methoxyphenyl)-imidazo[1,2-a]pyrimidine (280 mg, 80%) as a yellow solid. ^{1}H NMR (300 MHz, DMSO-d_6) δ 8.92 (dd, J = 6.6, 1.9 Hz, 1H), 8.50 (dd, J = 4.2, 1.8 Hz, 1H), 8.40 (d, J = 2.1 Hz, 1H), 8.34 (s, 1H), 7.99 (dd, J = 8.7, 2.2 Hz, 1H), 7.10 (d, J = 8.8 Hz, 1H), 7.03 (dd, J = 6.6, 4.2 Hz, 1H), 3.87 (s, 3H) (Fig. 1, top). ^{13}C NMR (75 Hz, DMSO-d_6) δ 158.5, 150.9, 148.7, 144.5, 136.8, 135.6, 128.7, 127.9, 112.5, 109.6, 107.7, 87.2, 57.2 (Fig. 1, bottom).

2-(2'-Iodo-4'methoxyphenyl)-imidazo[1,2-a]pyrimidine (280 mg, 0.797 mmol), isobutyramide (208.4 mg, 2.39 mmol), K_3PO_4 (338.4 mg, 1.594 mmol), CuI (15 mg, 80 micromol), *trans*-1,2-cyclohexyldiamine (19.5 microL, 159.4 micromoles) were combined, anhydrous 1,4-dioxane was added (1.5 mL) and the reaction was stirred under argon at 110°C for 18h. The reaction was cooled, filtered over celite, washed with EtOAc. The filtrate was washed with NH_4OH followed by sat NaCl, dried over Na_2SO_4, filtered and concentrated. Column chromatography (12g flash, 4 min. CH_2Cl_2, 4-10min gradient to 1:1 MeOH/CH_2Cl_2) gave CID 6622773 (115 mg, 47%) as a yellow solid. ^{1}H NMR (300 MHz, DMSO-d_6) δ 9.04 (s, 1H), 8.90 (dd, J = 6.7, 2.0 Hz, 1H), 8.57 (bs, 1H), 8.48 (dd, J = 4.1, 2.0 Hz, 1H), 8.24 (s, 1H), 7.70 (dd, J = 8.4, 2.0 Hz, 1H), 7.12 (d, J = 8.4 Hz, 1H), 7.02 (dd, J = 6.7, 4.1 Hz, 1H), 3.88 (s, 3H), 2.80 (m, 1H), 1.11 (d, J = 6.8 Hz, 6 H) (Fig. 2, top). ^{13}C NMR (75 Hz, DMSO-d_6) δ 175.4, 150.0, 149.8, 148.0, 145.5, 134.7, 127.6, 125.6, 121.7, 119.8, 111.3, 108.6, 106.5, 55.8, 34.5, 19.6 (Fig. 2, bottom). FTIR (KBr, cm^{-1}) 3423 (w), 3293 (m), 2965 (m), 1657 (s) (Fig. 3). HRMS *m/z* (ES+) calcd for $C_{17}H_{19}N_4O_2(M+H)^+$ 311.1508, found 311.1502 (Fig. 5)

LC-MS

CID 6622773 was eluted from a Waters Symmetry® C_{18} 5µm 3.0 X 150mm column with 83:17 CH_3CN/H_2O containing 0.01% formic acid, RT= 4.60 min. (Fig 4). UV-Vis at RT=4.60 min. λ_{max} 340nm (Fig. 5). ESI-MS *m/z* (ES+) calcd for $C_{17}H_{19}N_4O_2(M+H)^+$ 311.15, found 311.17 (Fig. 4).

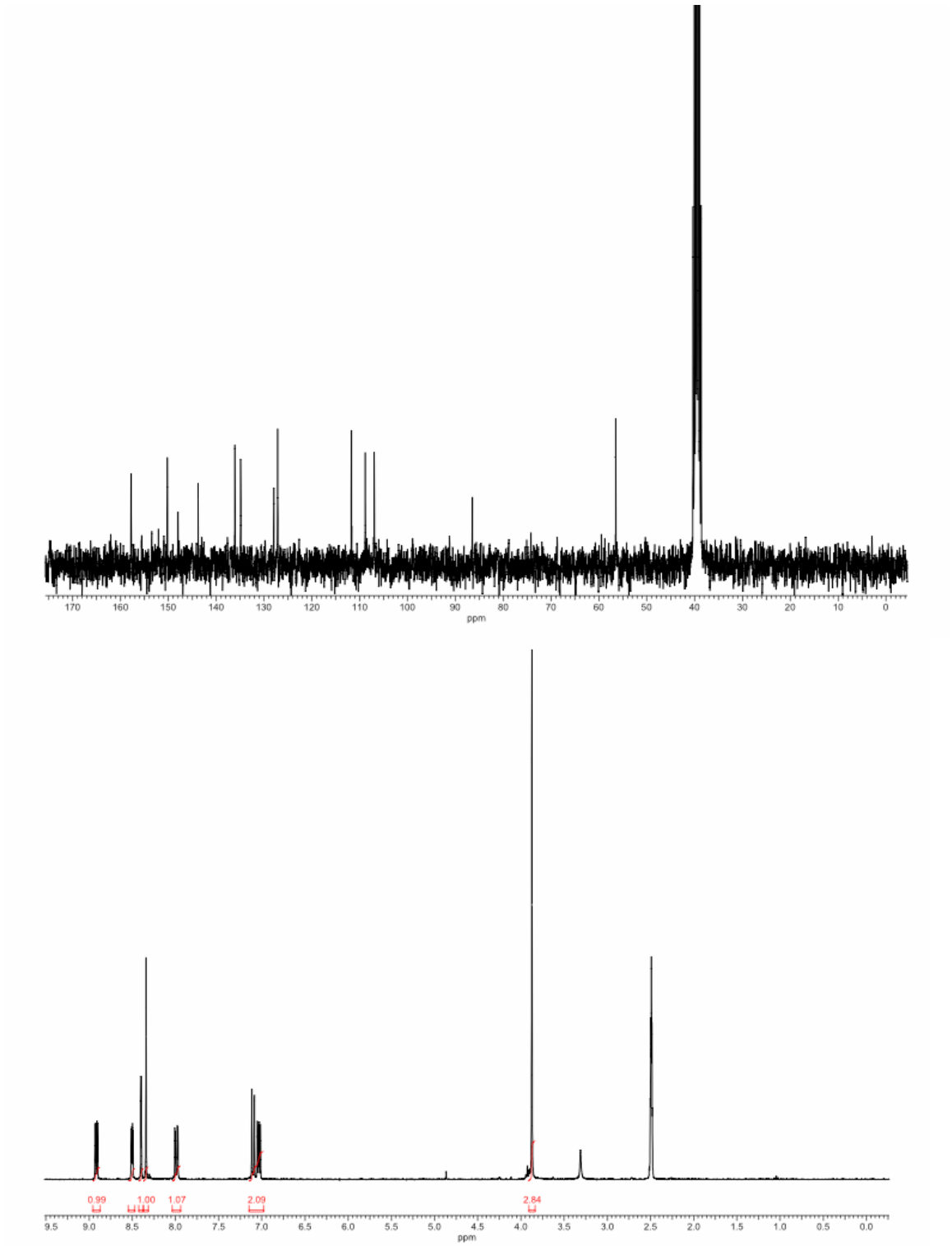

Fig. 1. ^{13}C NMR (top) and ^{1}H NMR (bottom) of 2-(2'Iodo-4'-methoxyphenyl)-imidazol(1,2-a)pyrimidine.

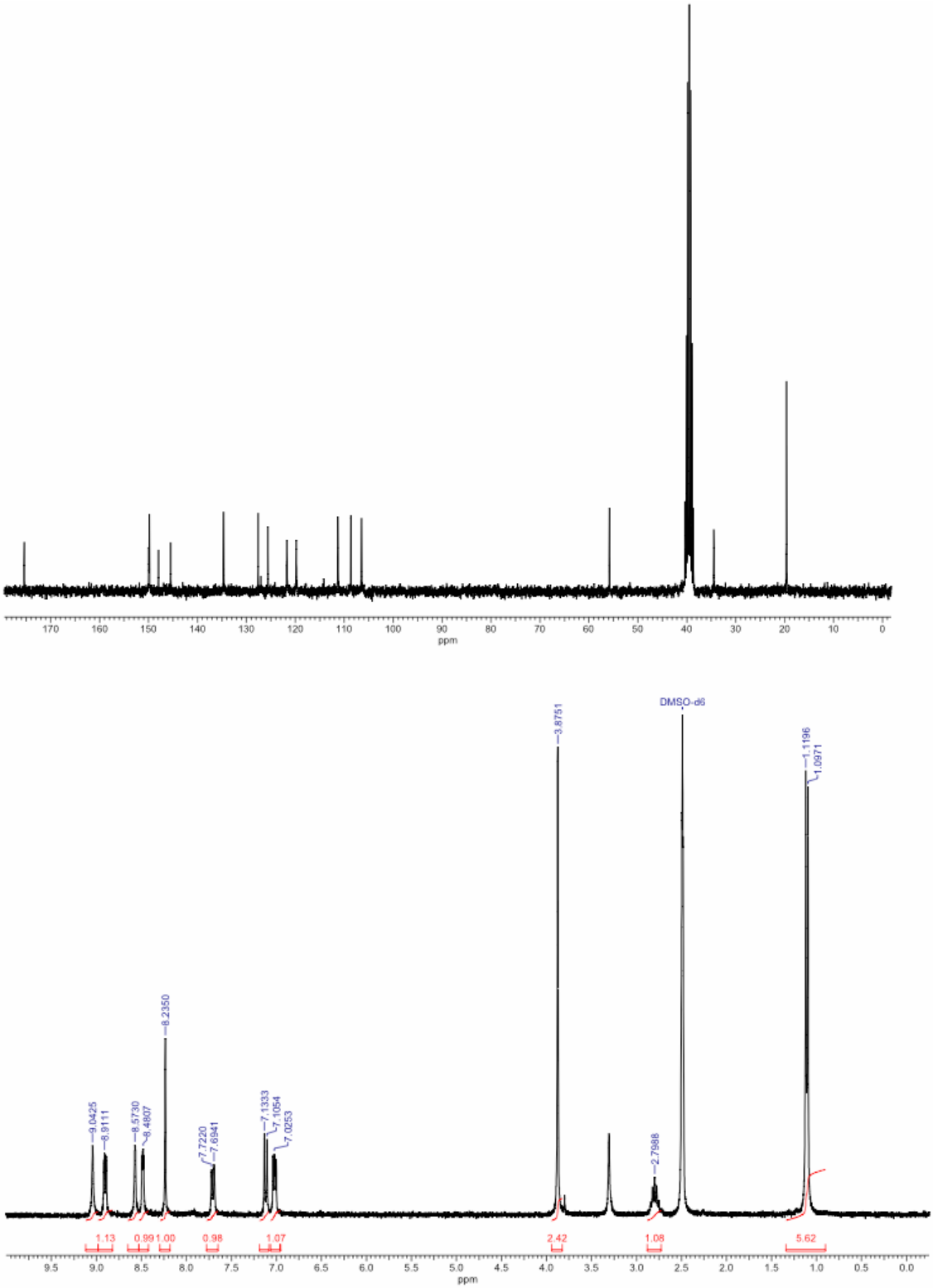

Fig. 2. ^{13}C NMR (top) and ^{1}H NMR (bottom) of BB-V-115 (CID 6622773).

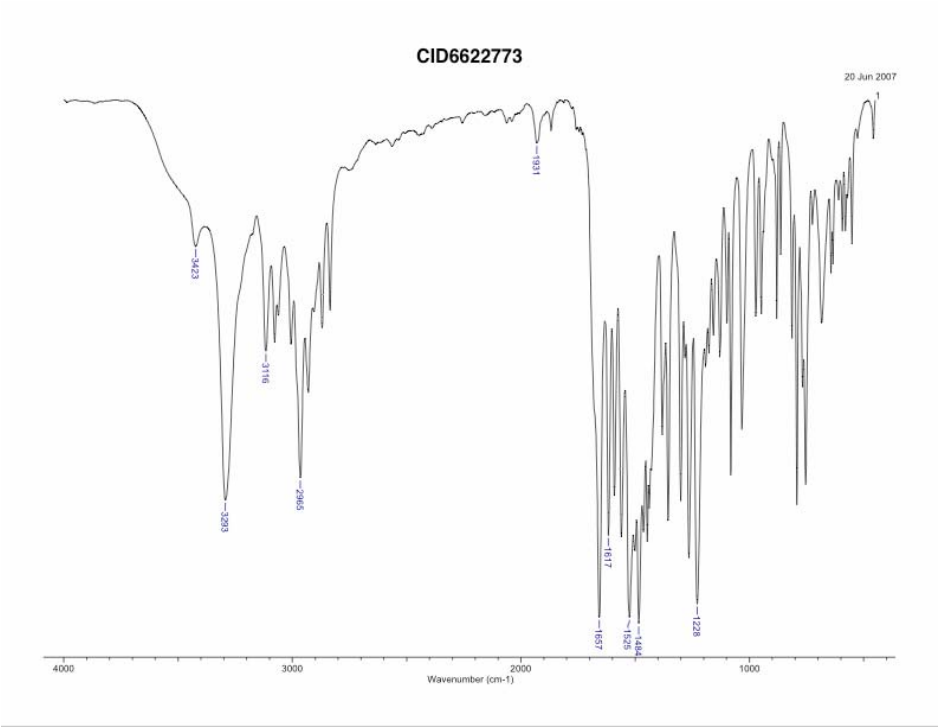

Fig. 3. FTIR Spectrum of BB-V-115 (CID 6622773)..

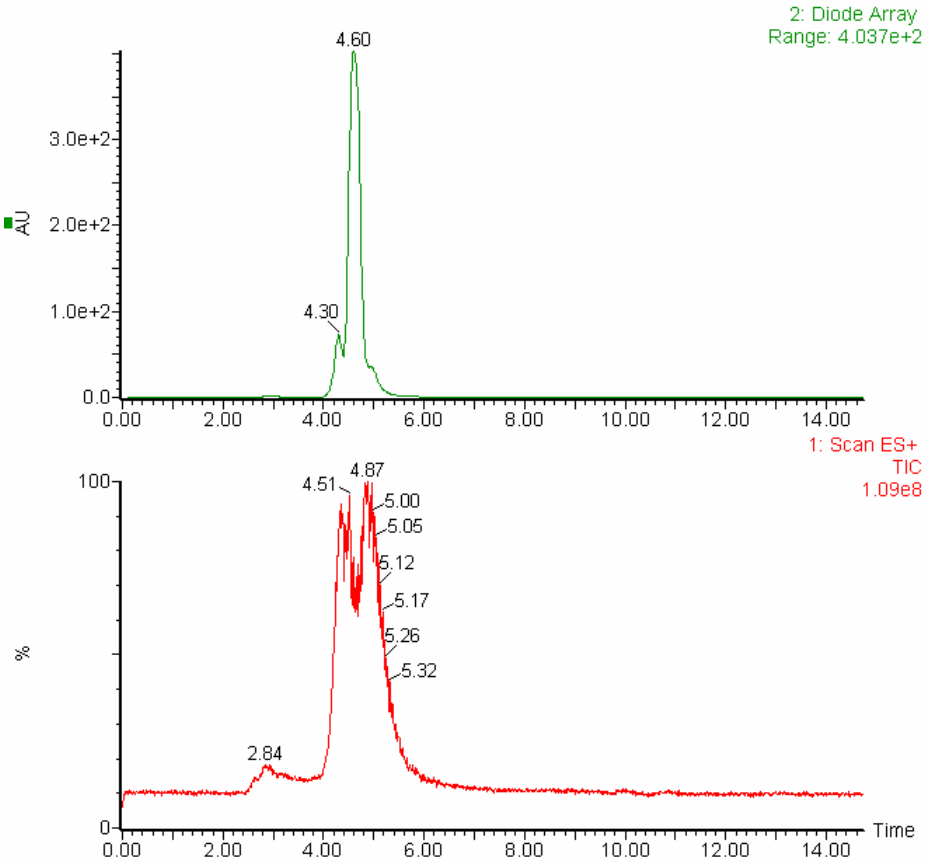

Fig. 4. HPLC PDA (top) and ESI-MS (ES+) TIC (bottom) of BB-V-115 (CID 6622773).

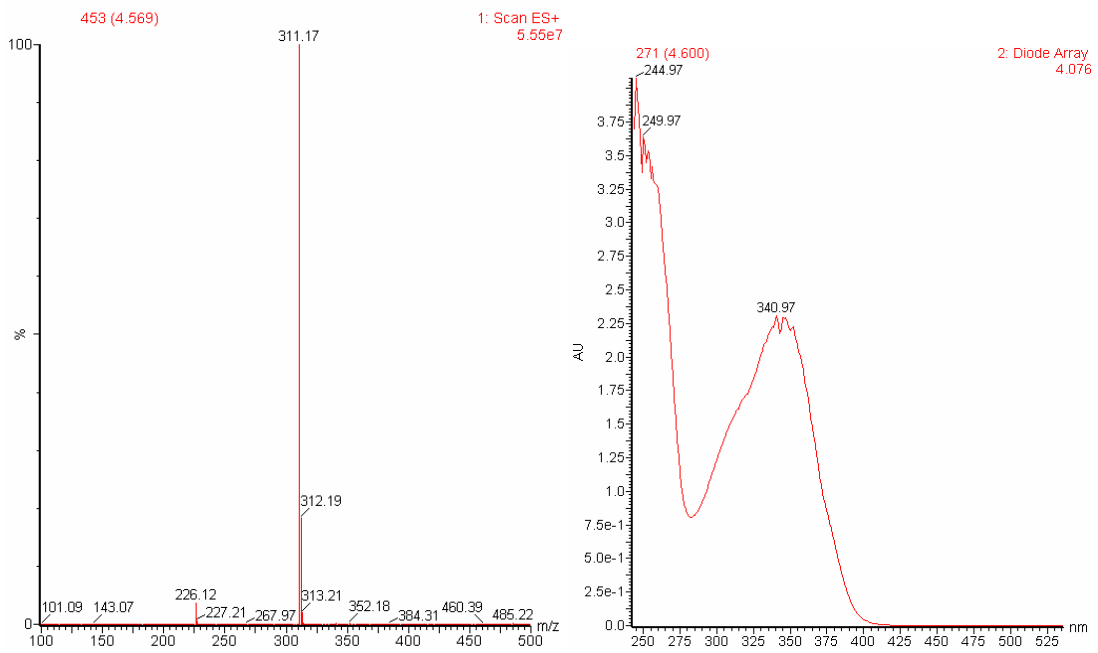

Fig. 5. HRMS (left) and UV-Vis (right) of BB-V-115 (CID 6622773).

Biological Characterization of the Resynthesized Probe

Binding to FPRL1. Dose response studies with the FPR-FPRL1 duplex ligand binding assay confirmed the potency of **BB-V-115**. In 17 dose response experiments performed in duplicate the K_i was determined to be 269 ± 51 nM (mean ± SEM). The IC_{50} was 1.01 ± 0.19 µM. Fig 6 illustrates pooled results of duplicate measurements from 3 of the 17 experiments in which BB-V-115 was compared with C7 in the same experiments. C7 is a recently reported small molecule FPRL1 antagonist (47) that we synthesized in our facility to enable such a direct comparison. In this set of experiments **BB-V-115** had a Ki of 174 nM (IC_{50} = 627 nM, Fig.6, left) while C7 had a Ki of 2.3 µM (IC_{50} = 8.4 µM, Fig. 6, right). Curve fit statistics for BB-V-115 (Fig. 6, left) indicated a Hill slope of 1.11 and an r^2 correlation coefficient of 0.95.

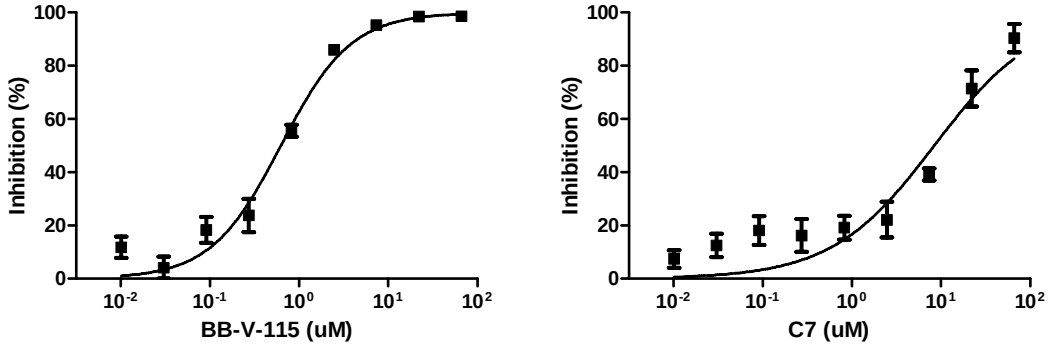

Fig. 6. **BB-V-115** and C7 inhibition of fluorescent ligand binding to FPRL1. Illustrated are pooled results of 3 experiments, each done in duplicate.

Counter Screen - Binding to FPR. In the parallel ligand displacement dose response experiments for FPR, done in the same wells as the FPRL1 ligand displacement experiments illustrated in Fig. 6, **BB-V-115** had a Ki of 3.5 μM (IC_{50} = 17.8 μM, Fig. 7, left) and C7 had a Ki of 3.2 μM (IC_{50} = 16.4 μM, Fig. 7, right). Thus, **BB-V-115** had 20-fold selectivity for FPRL1 vs FPR while C7 selectivity was only ~1.4-fold.

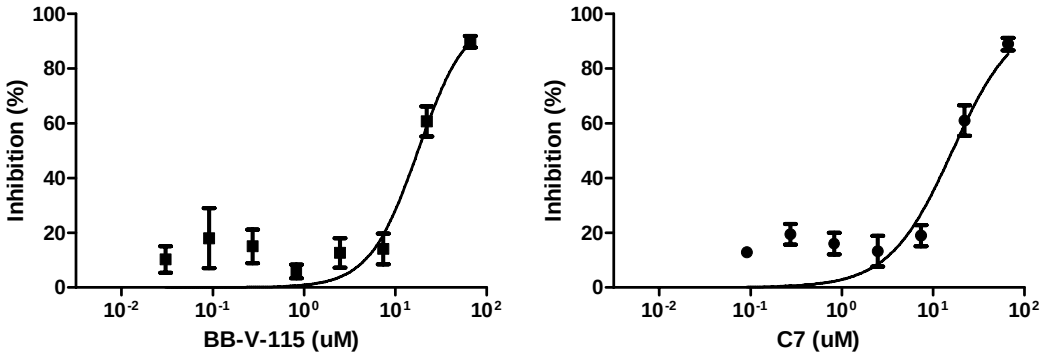

Fig. 7. **BB-V-115** and C7 effects on fluorescent ligand binding to FPR. Illustrated are pooled results of 3 experiments, each done in duplicate.

Secondary Intracellular Calcium Response Antagonist Assay. The resynthesized **BB-V-115** was confirmed to be an antagonist for intracellular calcium responses elicited in the presence of 1 nM WKYMVm (Fig. 8). The curve fit indicated an IC_{50} of 1.58 μM, Hill slope of 0.96, and r^2 correlation coefficient of 0.996. A 100 μM concentration of **BB-V-115** had no effect on the intracellular calcium response of U937 cells expressing the human FPR receptor in the presence of the FPR ligand, fMLFF (data not shown). Thus, **BB-V-115** is a selective FPRL1 antagonist.

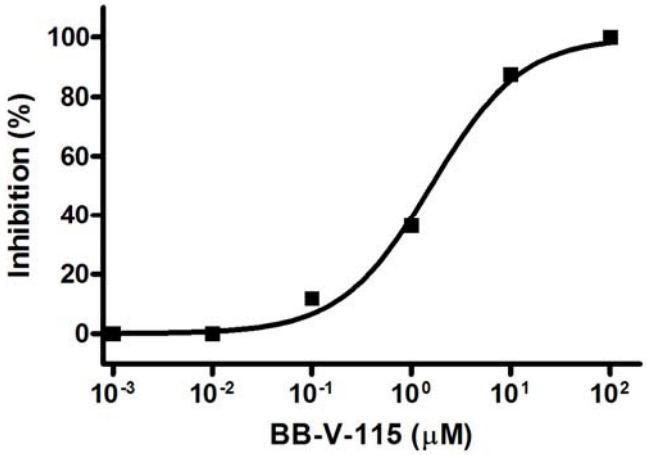

Fig. 8. **BB-V-115** antagonist activity for intracellular calcium response elicited by 1 nM WKYMVm.

FPRL1 Family 3 Structure Activity Relationship

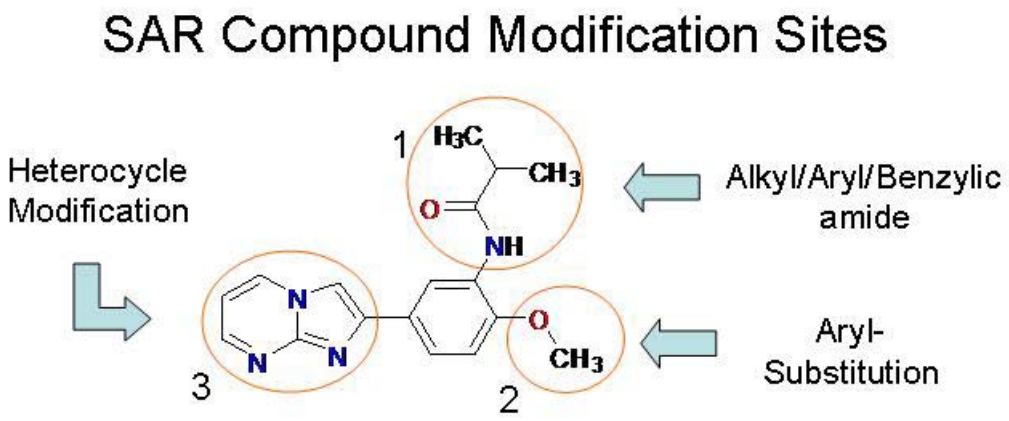

Fig. 9. **BB-V-115** modification sites for FPRL1 family 3 SAR. Regions 1-3 are indicated..

Three regions of FPRL1 family 1 structure were explored for SAR analysis (Fig. 9).

Region 1: All modifications for this region hold Regions 2 and 3 constant as shown above. Across subgroups, aryl amides showed no activity while alkyl and benzylic amides demonstrated a range of activities. No modification yielded an inhibition level as high as the parent compound.

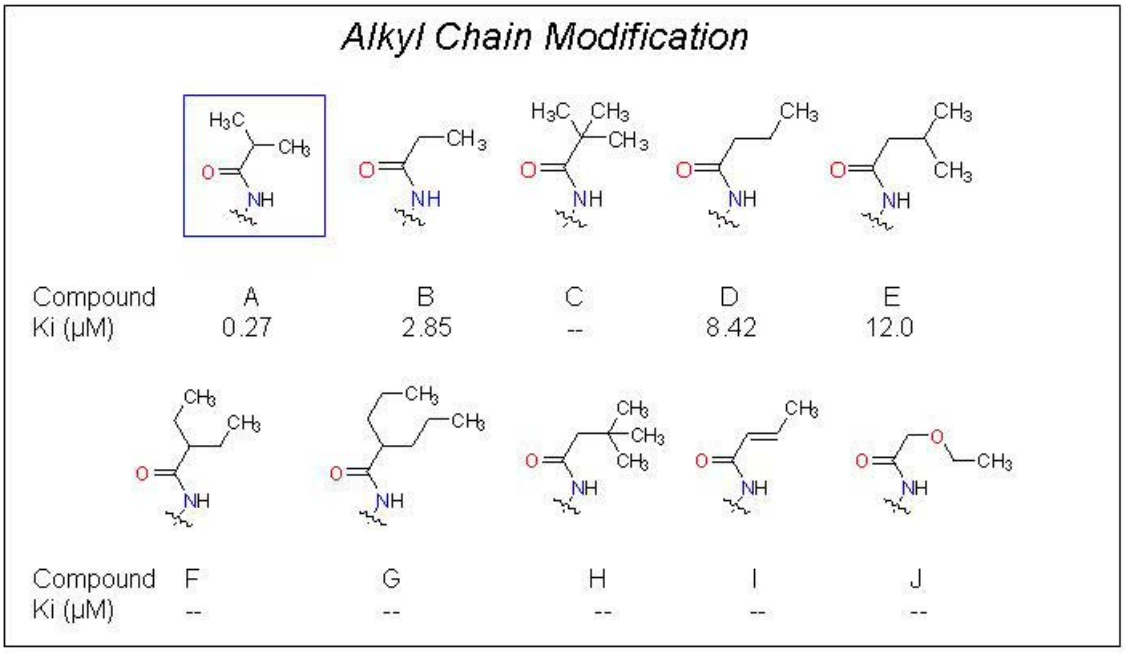

Fig. 10. Effect upon FPRL1 binding of alkyl chain modifications in Region 1. --, inactive in primary HTS screen or dose-response analysis.

Modification to the Region 1 amide with a variety of alkyl functional groups yielded less active substances as compared to the original hit (Fig. 10, blue box). A slight decrease in

the steric profile (isobutyramide A vs. propylamide B) resulted in a ten fold decrease in activity, however, increasing the steric profile led to significantly lower inhibitions, most of which were considered inactive. The unsaturated propenyl I was inactive as compared to it's saturated counterpart D (Fig. 10). The alkoxy amide analog J was also inactive (Fig 10).

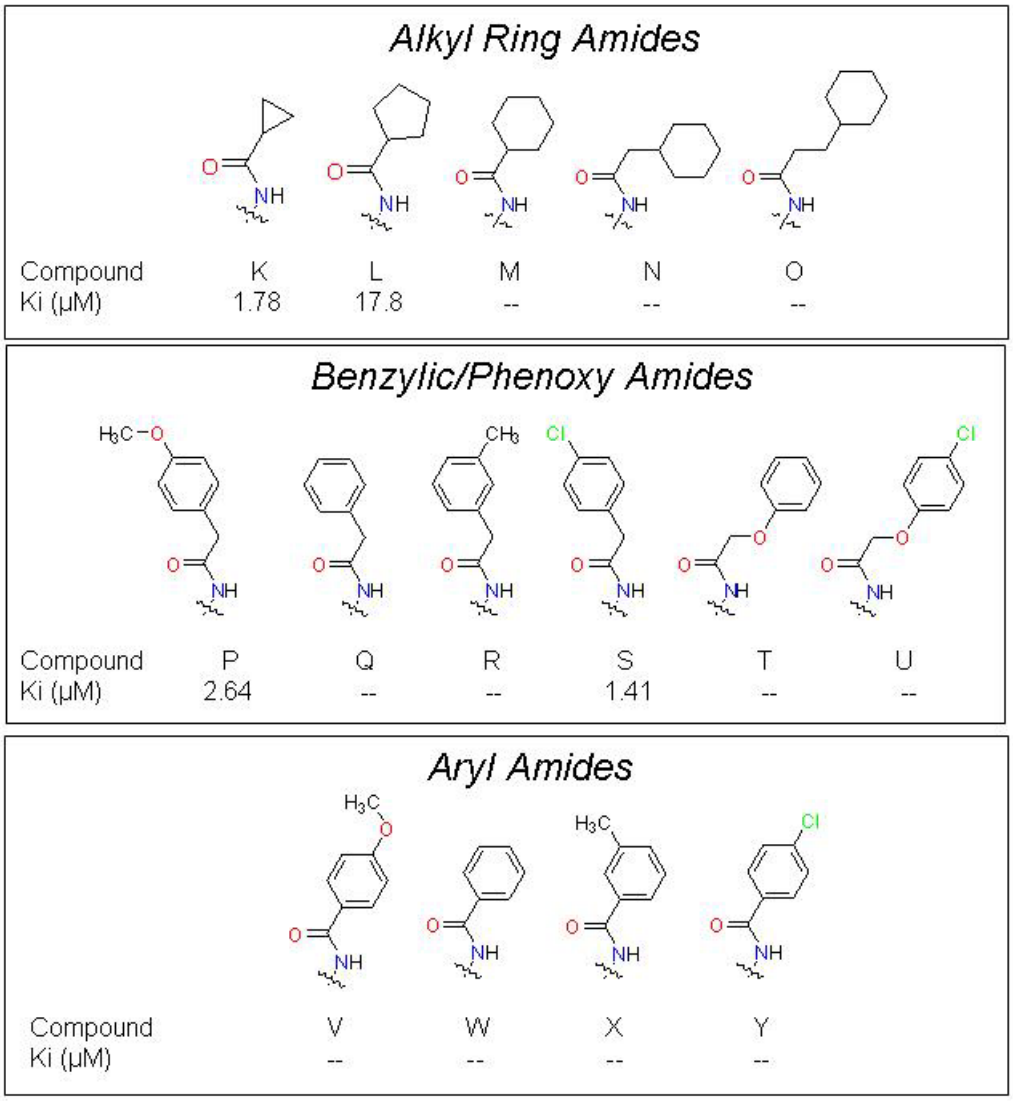

Fig. 11. Effects on FPRL1 binding activity of alkyl ring amides (top panel), benzylic and phenoxy amides (middle panel) and aryl amides (bottom panel).

In analysis of a series of alkyl amide substitutions in Region 1 (Fig 11, top panel), increasing ring size resulted in decreased activity with strongest inhibition by the ring closed (cyclopropyl) analog of the original hit. In a series of benzylic and phenoxy amide substitutions (Fig. 11, middle panel), both the electron rich P and electron deficient S showed similar inhibitions to that of the parent compound while the electroneutral Q and R showed no activity. The phenoxy analogs T and U were both inactive. All in a series of aryl amide substitutions were inactive (Fig. 11, bottom panel).

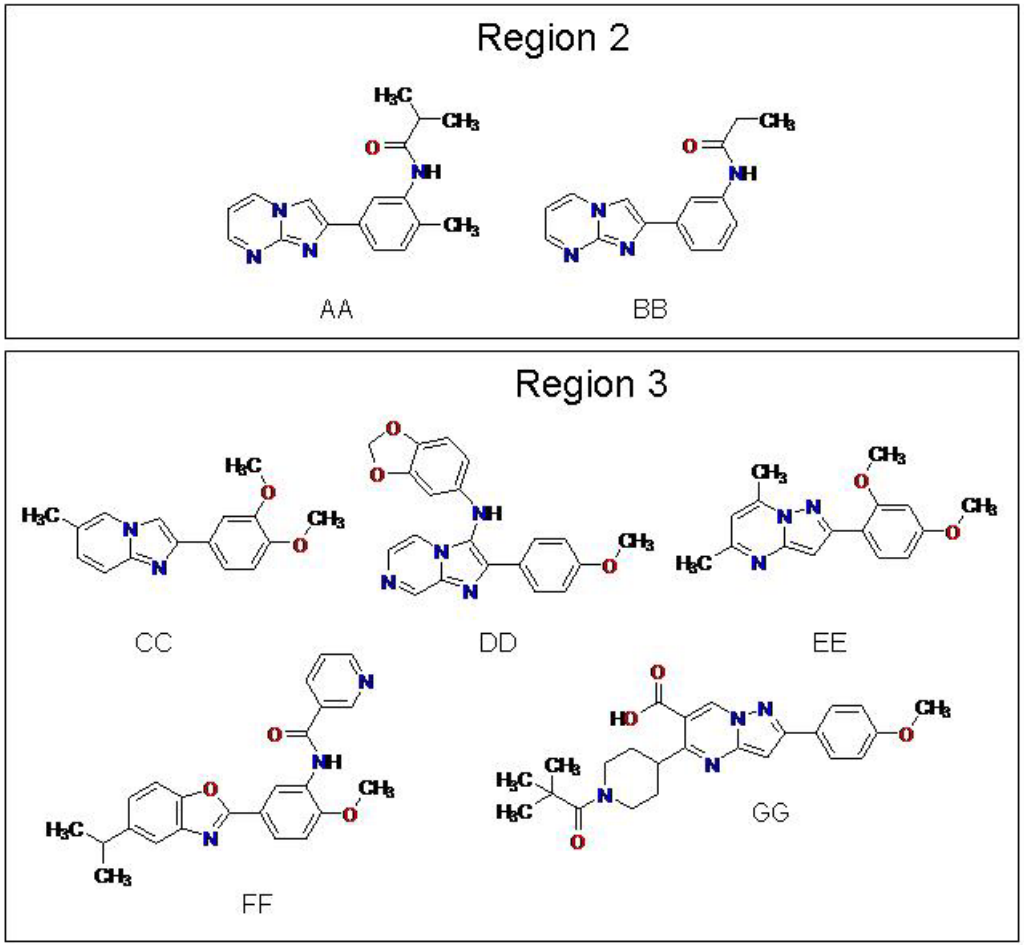

Fig. 12. SAR analysis of substitutions in Region 2 (top panel) and Region 3 (bottom panel) of **BB-V-115**.

Region 2: Modifications were limited at this region, but direct comparison to their methoxy counterparts was possible in both cases. In both compounds the change of the methoxy group led to inactivity in its counterpart (AA and BB in Fig. 12, top panel, vs. A and B in Fig. 10, respectively).

Region 3: A variety of similar structures was explored with modifications to the heterocyclic skeleton of the parent molecule, all of which were inactive. Direct comparison was not possible due to the presence of varied changes in other regions. A representative sample of these analogs is illustrated in Fig. 12, bottom panel.

Compounds referenced in SAR series illustrations (Fig. 10-12) are identified in Appendix tables below. All had undetectable activity against FPR in parallel assays performed as the complementary part of the assay duplex (PubChem AIDs 440, 519, 762 and 763).

References

1. Le, Y., Murphy, P. M., and Wang, J. M. Formyl-peptide receptors revisited. Trends Immunol, *23:* 541-548, 2002.
2. Oppenheim, J. J., Zachariae, C. O., Mukaida, N., and Matsushima, K. Properties of the novel proinflammatory supergene "intercrine" cytokine family. Annu Rev Immunol, *9:* 617-648, 1991.
3. Murphy, P. M. The N-formylpeptide chemotactic receptor. *In:* R. Horuk (ed.), Chemoattractant ligands and their receptors, pp. 269-299. Boca Raton, FL: CRC Press, 1996.
4. Le, Y., Oppenheim, J. J., and Wang, J. M. Pleiotropic roles of formyl peptide receptors. Cytokine Growth Factor Rev, *12:* 91-105, 2001.
5. Murphy, P. M. The molecular biology of leukocyte chemoattractant receptors. Annu Rev Immunol, *12:* 593-633, 1994.
6. He, R., Sang, H., and Ye, R. D. Serum amyloid A induces IL-8 secretion through a G protein-coupled receptor, FPRL1/LXA4R. Blood, *101:* 1572-1581, 2003.
7. Tiffany, H. L., Lavigne, M. C., Cui, Y. H., Wang, J. M., Leto, T. L., Gao, J. L., and Murphy, P. M. Amyloid-beta induces chemotaxis and oxidant stress by acting at formylpeptide receptor 2, a G protein-coupled receptor expressed in phagocytes and brain. J Biol Chem, *276:* 23645-23652, 2001.
8. Schiffmann, E., Showell, H. V., Corcoran, B. A., Ward, P. A., Smith, E., and Becker, E. L. The isolation and partial characterization of neutrophil chemotactic factors from Escherichia coli. J Immunol, *114:* 1831-1837, 1975.
9. Schiffmann, E., Corcoran, B. A., and Wahl, S. M. N-formylmethionyl peptides as chemoattractants for leucocytes. Proc Natl Acad Sci U S A, *72:* 1059-1062, 1975.
10. Marasco, W. A., Phan, S. H., Krutzsch, H., Showell, H. J., Feltner, D. E., Nairn, R., Becker, E. L., and Ward, P. A. Purification and identification of formyl-methionyl-leucyl-phenylalanine as the major peptide neutrophil chemotactic factor produced by Escherichia coli. J Biol Chem, *259:* 5430-5439, 1984.
11. Carp, H. Mitochondrial N-formylmethionyl proteins as chemoattractants for neutrophils. J Exp Med, *155:* 264-275, 1982.
12. Gao, J. L., Lee, E. J., and Murphy, P. M. Impaired antibacterial host defense in mice lacking the N-formylpeptide receptor. J Exp Med, *189:* 657-662, 1999.
13. Walther, A., Riehemann, K., and Gerke, V. A novel ligand of the formyl peptide receptor: annexin I regulates neutrophil extravasation by interacting with the FPR. Mol Cell, *5:* 831-840, 2000.
14. Zhou, Y., Bian, X., Le, Y., Gong, W., Hu, J., Zhang, X., Wang, L., Iribarren, P., Salcedo, R., Howard, O. M., Farrar, W., and Wang, J. M. Formylpeptide receptor FPR and the rapid growth of malignant human gliomas. J Natl Cancer Inst, *97:* 823-835, 2005.
15. Bao, L., Gerard, N. P., Eddy, R. L., Jr., Shows, T. B., and Gerard, C. Mapping of genes for the human C5a receptor (C5AR), human FMLP receptor (FPR), and two FMLP receptor homologue orphan receptors (FPRH1, FPRH2) to chromosome 19. Genomics, *13:* 437-440, 1992.
16. Murphy, P. M., Ozcelik, T., Kenney, R. T., Tiffany, H. L., McDermott, D., and Francke, U. A structural homologue of the N-formyl peptide receptor.

Characterization and chromosome mapping of a peptide chemoattractant receptor family. J Biol Chem, *267:* 7637-7643, 1992.
17. Ye, R. D., Cavanagh, S. L., Quehenberger, O., Prossnitz, E. R., and Cochrane, C. G. Isolation of a cDNA that encodes a novel granulocyte N-formyl peptide receptor. Biochem Biophys Res Commun, *184:* 582-589, 1992.
18. Nomura, H., Nielsen, B. W., and Matsushima, K. Molecular cloning of cDNAs encoding a LD78 receptor and putative leukocyte chemotactic peptide receptors. Int Immunol, *5:* 1239-1249, 1993.
19. Prossnitz, E. R. and Ye, R. D. The N-formyl peptide receptor: a model for the study of chemoattractant receptor structure and function. Pharmacol Ther, *74:* 73-102, 1997.
20. Su, S. B., Gong, W., Gao, J. L., Shen, W., Murphy, P. M., Oppenheim, J. J., and Wang, J. M. A seven-transmembrane, G protein-coupled receptor, FPRL1, mediates the chemotactic activity of serum amyloid A for human phagocytic cells. J Exp Med, *189:* 395-402, 1999.
21. Le, Y., Gong, W., Tiffany, H. L., Tumanov, A., Nedospasov, S., Shen, W., Dunlop, N. M., Gao, J. L., Murphy, P. M., Oppenheim, J. J., and Wang, J. M. Amyloid (beta)42 activates a G-protein-coupled chemoattractant receptor, FPR-like-1. J Neurosci, *21:* RC123, 2001.
22. Le, Y., Yazawa, H., Gong, W., Yu, Z., Ferrans, V. J., Murphy, P. M., and Wang, J. M. The neurotoxic prion peptide fragment PrP(106-126) is a chemotactic agonist for the G protein-coupled receptor formyl peptide receptor-like 1. J Immunol, *166:* 1448-1451, 2001.
23. Snipe, J. D. The acute phase response. *In:* E. M. Shevac (ed.), Immunophysiology: the role of cells and cytokines in immunity and inflammation, pp. 259-273. New York, NY: Oxford University Press, 1990.
24. Lambert, M. P., Barlow, A. K., Chromy, B. A., Edwards, C., Freed, R., Liosatos, M., Morgan, T. E., Rozovsky, I., Trommer, B., Viola, K. L., Wals, P., Zhang, C., Finch, C. E., Krafft, G. A., and Klein, W. L. Diffusible, nonfibrillar ligands derived from Abeta1-42 are potent central nervous system neurotoxins. Proc Natl Acad Sci U S A, *95:* 6448-6453, 1998.
25. Kalaria, R. N. Microglia and Alzheimer's disease. Curr Opin Hematol, *6:* 15-24, 1999.
26. Brown, D. R., Schmidt, B., and Kretzschmar, H. A. Role of microglia and host prion protein in neurotoxicity of a prion protein fragment. Nature, *380:* 345-347, 1996.
27. Le, Y., Yang, Y., Cui, Y., Yazawa, H., Gong, W., Qiu, C., and Wang, J. M. Receptors for chemotactic formyl peptides as pharmacological targets. Int Immunopharmacol, *2:* 1-13, 2002.
28. Yazawa, H., Yu, Z. X., Takeda, Le, Y., Gong, W., Ferrans, V. J., Oppenheim, J. J., Li, C. C., and Wang, J. M. Beta amyloid peptide (Abeta42) is internalized via the G-protein-coupled receptor FPRL1 and forms fibrillar aggregates in macrophages. Faseb J, *15:* 2454-2462, 2001.
29. De, Y., Chen, Q., Schmidt, A. P., Anderson, G. M., Wang, J. M., Wooters, J., Oppenheim, J. J., and Chertov, O. LL-37, the neutrophil granule- and epithelial cell-derived cathelicidin, utilizes formyl peptide receptor-like 1 (FPRL1) as a

receptor to chemoattract human peripheral blood neutrophils, monocytes, and T cells. J Exp Med, *192:* 1069-1074, 2000.
30. Chiang, N., Fierro, I. M., Gronert, K., and Serhan, C. N. Activation of lipoxin A(4) receptors by aspirin-triggered lipoxins and select peptides evokes ligand-specific responses in inflammation. J Exp Med, *191:* 1197-1208, 2000.
31. Su, S. B., Gao, J., Gong, W., Dunlop, N. M., Murphy, P. M., Oppenheim, J. J., and Wang, J. M. T21/DP107, A synthetic leucine zipper-like domain of the HIV-1 envelope gp41, attracts and activates human phagocytes by using G-protein-coupled formyl peptide receptors. J Immunol, *162:* 5924-5930, 1999.
32. Le, Y., Jiang, S., Hu, J., Gong, W., Su, S., Dunlop, N. M., Shen, W., Li, B., and Ming Wang, J. N36, a synthetic N-terminal heptad repeat domain of the HIV-1 envelope protein gp41, is an activator of human phagocytes. Clin Immunol, *96:* 236-242, 2000.
33. VanCompernolle, S. E., Clark, K. L., Rummel, K. A., and Todd, S. C. Expression and function of formyl peptide receptors on human fibroblast cells. J Immunol, *171:* 2050-2056, 2003.
34. Durstin, M., Gao, J. L., Tiffany, H. L., McDermott, D., and Murphy, P. M. Differential expression of members of the N-formylpeptide receptor gene cluster in human phagocytes. Biochem Biophys Res Commun, *201:* 174-179, 1994.
35. McCoy, R., Haviland, D. L., Molmenti, E. P., Ziambaras, T., Wetsel, R. A., and Perlmutter, D. H. N-formylpeptide and complement C5a receptors are expressed in liver cells and mediate hepatic acute phase gene regulation. J Exp Med, *182:* 207-217, 1995.
36. Sozzani, S., Sallusto, F., Luini, W., Zhou, D., Piemonti, L., Allavena, P., Van Damme, J., Valitutti, S., Lanzavecchia, A., and Mantovani, A. Migration of dendritic cells in response to formyl peptides, C5a, and a distinct set of chemokines. J Immunol, *155:* 3292-3295, 1995.
37. Lacy, M., Jones, J., Whittemore, S. R., Haviland, D. L., Wetsel, R. A., and Barnum, S. R. Expression of the receptors for the C5a anaphylatoxin, interleukin-8 and FMLP by human astrocytes and microglia. J Neuroimmunol, *61:* 71-78, 1995.
38. Keitoku, M., Kohzuki, M., Katoh, H., Funakoshi, M., Suzuki, S., Takeuchi, M., Karibe, A., Horiguchi, S., Watanabe, J., Satoh, S., Nose, M., Abe, K., Okayama, H., and Shirato, K. FMLP actions and its binding sites in isolated human coronary arteries. J Mol Cell Cardiol, *29:* 881-894, 1997.
39. Gronert, K., Gewirtz, A., Madara, J. L., and Serhan, C. N. Identification of a human enterocyte lipoxin A4 receptor that is regulated by interleukin (IL)-13 and interferon gamma and inhibits tumor necrosis factor alpha-induced IL-8 release. J Exp Med, *187:* 1285-1294, 1998.
40. Le, Y., Hu, J., Gong, W., Shen, W., Li, B., Dunlop, N. M., Halverson, D. O., Blair, D. G., and Wang, J. M. Expression of functional formyl peptide receptors by human astrocytoma cell lines. J Neuroimmunol, *111:* 102-108, 2000.
41. Nanamori, M., Cheng, X., Mei, J., Sang, H., Xuan, Y., Zhou, C., Wang, M. W., and Ye, R. D. A novel nonpeptide ligand for formyl peptide receptor-like 1. Mol Pharmacol, *66:* 1213-1222, 2004.
42. Burli, R. W., Xu, H., Zou, X., Muller, K., Golden, J., Frohn, M., Adlam, M., Plant, M. H., Wong, M., McElvain, M., Regal, K., Viswanadhan, V. N., Tagari,

P., and Hungate, R. Potent hFPRL1 (ALXR) agonists as potential anti-inflammatory agents. Bioorg Med Chem Lett, *16:* 3713-3718, 2006.

43. Kuckuck, F. W., Edwards, B. S., and Sklar, L. A. High throughput flow cytometry. Cytometry, *44:* 83-90, 2001.
44. Ramirez, S., Aiken, C. T., Andrzejewski, B., Sklar, L. A., and Edwards, B. S. High-throughput flow cytometry: Validation in microvolume bioassays. Cytometry, *53A:* 55-65, 2003.
45. Munson, P. J. and Rodbard, D. An exact correction to the "Cheng-Prusoff" correction. J Recept Res, *8:* 533-546, 1988.
46. Young, S. M., Curry, M. S., Ransom, J. T., Ballesteros, J. A., Prossnitz, E. R., Sklar, L. A., and Edwards, B. S. High-throughput microfluidic mixing and multiparametric cell sorting for bioactive compound screening. J Biomol Screen, *9:* 103-111, 2004.
47. Zhou, C., Zhang, S., Nanamori, M., Zhang, Y., Liu, Q., Li, N., Sun, M., Tian, J., Ye, P. P., Cheng, N., Ye, R. D., and Wang, M. W. Pharmacological characterization of a novel nonpeptide antagonist for formyl peptide receptor-like 1. Mol Pharmacol, *72:* 976-983, 2007.

Appendix

Com-pound	SID	CID	Structure	Ki (M)
A	24702504	6622773	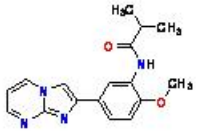	2.690E-7
B	24702503	7080248		2.85E-6
C	24702505	7080249	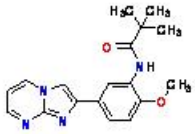	-----
D	24702397	3245971	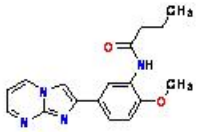	8.42E-6
E	4250964	3244709	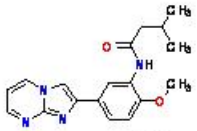	1.20E-5
F	24702506	7080251	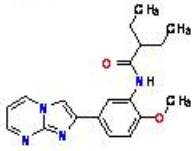	-----
G	24702507	7080252	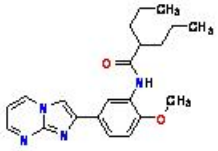	-----
H	24702505	7080249	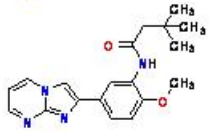	-----
I	24702500	16061401	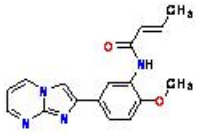	-----

Com-pound	SID	CID	Structure	Ki (M)
J	24702511	7080256	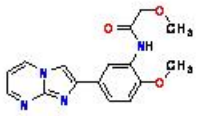	-----
K	24702398	3236767	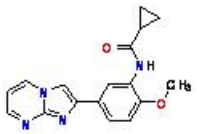	1.78E-6
L	4241155	3236168	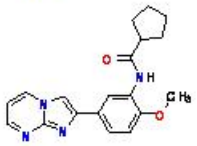	1.78E-5
M	24702508	7080253	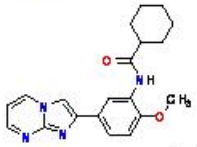	-----
N	24702509	7080254	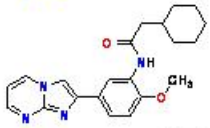	-----
O	24702510	7080255	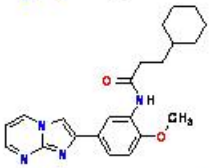	-----
P	24702546	7080289	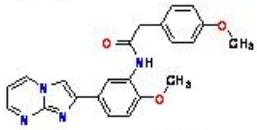	2.64E-6
Q	24702545	16031820	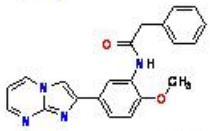	-----
R	24702548	7080291		-----
S	24702547	7080290		1.41E-6

Com-pound	SID	CID	Structure	Ki (M)
T	24702541	7080284	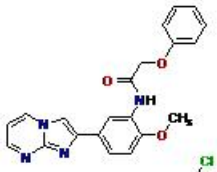	-----
U	24702542	7080285	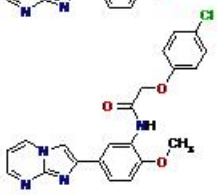	-----
V	24702519	7080265	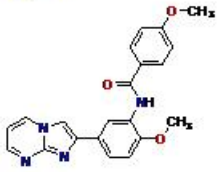	-----
W	24702512	6462848	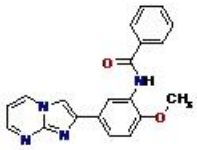	-----
X	24702513	7080258	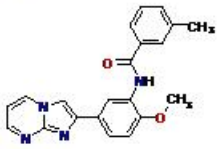	-----
Y	24702530	5304381	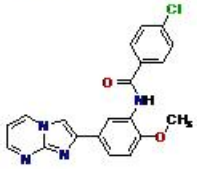	-----
AA	24702502	7080192	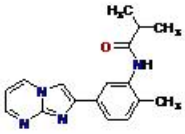	-----
BB	24702501	6622771	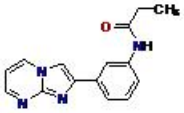	-----

Com-pound	SID	CID	Structure	Ki (M)
CC	3711876	6602984	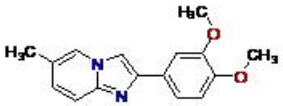	-----
DD	7969285	5309877	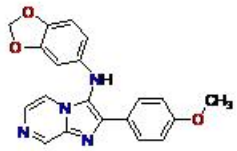	-----
EE	4249421	3243378	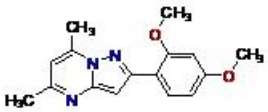	-----
FF	4264213	1305251	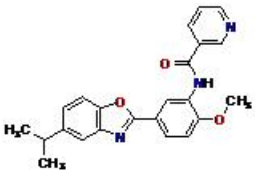	-----
GG	4246614	3240935	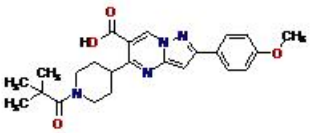	-----